Linear response of east Greenland's tidewater glaciers to ocean/atmosphere warming

T.R. Cowton*[1], A.J. Sole[2], P.W. Nienow[3], D.A. Slater[4] and P. Christoffersen[5]

*corresponding author

[1]School of Geography and Sustainable Development, University of St Andrews, KY16 9AL, UK

[2]Department of Geography, University of Sheffield, S10 2TN, UK

[3]School of Geosciences, University of Edinburgh, EH8 9XP, UK

[4]Scripps Institute of Oceanography, UC San Diego, La Jolla, CA 92093, USA

[5]Scott Polar Research Institute, University of Cambridge, CB2 1ER, UK

Abstract

Predicting the retreat of tidewater outlet glaciers forms a major obstacle to forecasting the rate of mass loss from the Greenland Ice Sheet. This reflects the challenges of modelling the highly dynamic, topographically complex and data poor environment of the glacier–fjord systems that link the ice sheet to the ocean. To avoid these difficulties, we investigate the extent to which tidewater glacier retreat can be explained by simple variables: air temperature, meltwater runoff, ocean temperature, and two simple parameterisations of 'ocean/atmosphere' forcing based on the combined influence of runoff and ocean temperature. Over a 20-year period at 10 large tidewater outlet glaciers along the east coast of Greenland, we find that ocean/atmosphere forcing can explain up to 76 % of the variability in terminus position at individual glaciers and 54 % of variation in terminus position across all 10 glaciers. Our findings indicate that 1) the retreat of east Greenland's tidewater glaciers is best explained as a product of both oceanic and atmospheric warming and 2) despite the complexity of tidewater glacier behaviour, over multi-year time scales a significant proportion of terminus position change can be explained as a simple function of this forcing. These findings thus demonstrate that simple parameterisations can play an important role in predicting the response of the ice sheet to future climate warming.

Significance statement

Mass loss from the Greenland Ice Sheet is expected to be a major contributor to 21st Century sea level rise, but projections retain substantial uncertainty due to the challenges of modelling the retreat of the tidewater outlet glaciers that drain from the ice sheet into the ocean. Despite the complexity of these glacier-fjord systems, we find that over a 20-year period much of the observed tidewater glacier retreat can be explained as a predictable response to combined atmospheric and oceanic warming, bringing us closer to incorporating these effects into the ice sheet models used to predict sea level rise.

Introduction

Loss of mass from tidewater glaciers to the ocean through iceberg calving and submarine melting is a major component of the mass budget of the Greenland Ice Sheet (GrIS). The contribution of this *frontal ablation* to ice sheet mass balance can vary dramatically on short timescales: increased frontal ablation was responsible for 39 % of GrIS mass loss from 1991-2015 (van den Broeke et al., 2017), and accounted for as much as two thirds of GrIS mass loss during a phase of rapid retreat, acceleration and thinning of outlet glaciers between 2000-05 (Rignot and Kanagaratnam, 2006). Understanding the controls on frontal ablation is thus crucial if its contribution to the mass budget of the GrIS is to be predicted by models (e.g. Nick et al., 2013).

Frontal ablation and tidewater glacier retreat are closely interlinked – if ice loss at the terminus is more rapid than the delivery of ice from up-glacier, the terminus will retreat. A leading hypothesis attributes the recent rapid retreat of many of Greenland's tidewater glaciers to an increase in submarine melting, and consequently calving, in response to oceanic warming (e.g. Straneo and Heimbach, 2013). Alternatively, retreat may have been driven by increasing surface melt, with meltwater runoff draining through glaciers and entering fjords at depth to form buoyant plumes which enhance submarine melting at glacier termini (e.g. Jenkins, 2011, Fried et al., 2015). It has also been suggested that increased surface melt and runoff may accelerate calving through hydrofracturing of near-terminus crevasses (e.g. Nick et al., 2013), or by increasing basal water pressure and hence basal motion (e.g. Sugiyama et al., 2011). A third hypothesis links retreat to increased calving rates following a reduction in terminus buttressing by ice mélange and land-fast sea ice (e.g. Christoffersen et al., 2012, Moon et al., 2015). In most cases however, it has not proven possible to attribute observed variability in terminus position to a particular cause, especially when multiple glaciers are considered (e.g. McFadden et al., 2011, Bevan et al., 2012, Carr et al., 2013, Moon et al., 2015, Murray et al., 2015).

The lack of a clear relationship between observed tidewater glacier retreat and changing environmental conditions presents a significant issue for modelling studies which seek to predict mass loss from the GrIS under a warming climate (e.g. Goelzer et al., 2013, Fürst et al., 2015). One challenge in establishing a causal relationship between environmental forcings and tidewater glacier retreat is that at the scale of individual glaciers these relationships often appear highly nonlinear, with feedbacks triggered as the terminus retreats across uneven bed topography obscuring the forcing driving the initial retreat (e.g. Vieli et al., 2002). This difficulty is compounded by a poor understanding of the oceanic forcing of these glaciers, due both to the scarcity of observations and the complexities of calving and submarine melt processes at glacier termini (Straneo et al., 2013). A further issue is that accurately representing these processes in ice sheet and ocean models would require model resolution and a knowledge of boundary conditions that lies beyond current capabilities (Benn et al., 2017).

In this paper, we seek to address these challenges to improve our understanding of the retreat of Greenland's tidewater glaciers on timescales relevant to predictions of mass loss over coming decades. We focus our study on 10 tidewater glaciers along Greenland's east coast of varying size and spanning > 10° of latitude (Table S1; Figure 1). Over a 20-year period (1993-2012) we compare the observed pattern and rate of retreat with variability in five environmental forcings, assessing the ability of these forcings to explain variability in the terminus position (P) of the study glaciers, both individually and collectively. These forcings comprise near-terminus air temperature (T_A), glacier meltwater runoff (Q), ocean temperature (T_O) and two parameterisations of combined 'ocean/atmosphere' forcing (M_1 and M_2). These ocean/atmosphere forcing parameterisations reflect the theory that frontal ablation will depend not only on ocean temperature but also runoff due to its role in stimulating buoyant upwelling adjacent to the terminus (e.g. Jenkins, 2011, Chauché et al., 2014) and driving the renewal of warm water in the fjord (e.g. Cowton et al., 2016, Carroll et al., 2017), thereby increasing the transfer of heat between the ocean and ice. To represent this combined ocean/atmosphere forcing we define $M_1 = Q(T_O-T_f)$ and $M_2 = Q^{1/3}(T_O-T_f)$. In these parameterisations, ocean temperature is expressed relative to the *in situ* freezing point at the calving front, approximated as T_f = -2.13 °C based on a depth of 300 m and salinity of 34.5 psu (e.g. Straneo et al., 2012). M_1 is thus a simple product of runoff and the oceanic heat available for melting, while the addition of the exponent to the formulation for M_2 is based on the expectation that submarine melt rate will scale linearly with temperature and with runoff raised to the power of 1/3 (Jenkins, 2011).

Results

Time series of variability in T_A, Q, T_O and P for each of the study glaciers are plotted in Figure 2 (see also Methods). These time series, along with the two ocean/atmosphere forcings M_1 and M_2, are displayed as normalised values for each glacier in Figure 3. Glaciers are grouped into 'northern' and 'southern' subsets based on their location with respect to a steep latitudinal gradient in ocean temperature at ~69° N, which reflects the influence of the Irminger Current (Seale et al., 2011; Figure 1). Features specific to the individual glaciers (in particular, fjord and subglacial topography) may modify their response to environmental forcings (e.g. Carr et al., 2013), and so the normalised values are also averaged for the five southern and five northern glaciers to show the regional trends, thereby emphasising the climatic signal (Figure 3f,l).

We begin by examining the relationship between terminus position and the environmental forcings at the scale of individual glaciers. At the southern glaciers, there is a marked increase in the values of the forcings and retreat of the glaciers between 2000 and 2005, with periods of relative stability either side (Figures 2 and 3a-f). There are strong correlations between P and the forcings (R^2 = 0.24-0.76, depending on the glacier and forcing; Figure 4, Table S2) for both the individual glaciers and regional trends. Because the time series involved are non-stationary, there is however an increased risk of spurious correlations resulting from similar long-term trends in the forcing and response variables existing over the study period (Granger and Newbold, 1974). We therefore run an Engle-Granger test for cointegration (Engle and Granger, 1987), which facilitates statistical comparison between two (or more) non-stationary time series showing stochastic trends (Methods). We find that P is significantly cointegrated ($p < 0.05$) with Q and M_1 at all of the southern study glaciers, with T_A and T_O at Mogens 3 (M3), AP Bernstorffs Glacier (AB) and Helheim Glacier (HG), and with M_2 at AB and HG (Figure 4, Table S2). Cointegration indicates a temporally-constant functional relationship, meaning that these results support the existence of causal relationships between P and the environmental forcings. However, because the forcings demonstrate similar temporal variability to each other, determining which (if any) is the key control on terminus position from this analysis alone remains difficult.

The results are qualitatively similar at the northern glaciers, which show a brief retreat during a phase of higher T_A, Q and T_O (and thus also M_1 and M_2) between ~1994-1995, then a slight re-advance, before embarking on a more sustained retreat in keeping with the increase in the forcings after ~2001 (Figure 3g-l). The statistical significance of these trends is however weaker at the northern glaciers (Figure 4 and Table S2), with significant cointegration of P with all forcings at Daugaard-Jensen Glacier (DJ) and with M_1 and M_2 at Waltershausen Glacier (WG). This may be due in part to the smaller absolute variability in the time series at the northern glaciers, increasing the magnitude of short-term noise relative to the long-term trends (Figures 2 and 3). Nevertheless, clear similarities appear between the variability in the forcings in P when the normalised data from the northern glaciers are combined to show the regional trends (Figure 3l). Correlation of the individual forcings and P for the combined northern glaciers data sets give R^2 values of 0.51-0.63 (significant at $p < 0.01$, Figure 4, Table S2); however, only M_1 is significantly cointegrated with P at $p < 0.05$.

This analysis indicates that, despite the complexities introduced by bed topography and ice dynamics, over timescales of a few years or more many individual glaciers display a largely linear response to environmental forcings. This is particularly apparent at the southern glaciers, where both the increase in forcings and glacier retreat have been more pronounced (Figures 2 and 3). However, because at this level P demonstrates strong correlations with multiple forcings, it remains unclear whether this retreat has been driven primarily by warming of the atmosphere, ocean, or both. To gain further insight, we therefore examine variation in glacier retreat across all 10 study glaciers.

Any environmental control on P should also be able to explain variation in retreat rate between glaciers. In particular, the absolute magnitude of retreat is consistently lower at the northern compared to the southern glaciers (with the standard deviation in P at the northern glaciers just 17 % of that exhibited at the southern glaciers), a trend which remains true for an expanded sample of 32 of east Greenland's tidewater glaciers (Seale et al., 2011). When the absolute variability at all glaciers is considered together, there is a significant ($p < 0.01$) correlation of P with Q (Figure 5a; R^2 = 0.40), T_O (Figure 5b; R^2 = 0.36) and T_A (Figure 5a; R^2 = 0.21). However, while T_A, Q *and* T_O are all typically higher at the southern than the northern glaciers, the latitudinal difference in the magnitude of the variability is less marked compared to that in P: the standard deviation in Q, T_O and T_A at the northern glaciers is 60, 74 and 93 % respectively of the standard deviation at the southern glaciers. The implication is that for a given change in these forcings, the southern glaciers have responded more sensitively than the northern glaciers. Combining Q and T to create M_1 and M_2 increases the latitudinal gradient in the forcings to give better agreement with that observed in P, with the standard deviation in both M_1 and M_2 at the northern glaciers 36 % of that exhibited at the southern glaciers. Combined with a good correlation at the glacier level (Figure 4), this helps to strengthen the correlation *of* P with M_1 (Figure 5c; R^2 = 0.54), and to a lesser extent the slightly more complex ocean/atmosphere forcing parameter M_2 (Figure 5d; R^2= 0.45).

We additionally test the ability of the environmental forcings to explain only the inter-glacier variability in long-term retreat rate, a property of arguably greater importance than the year-to-year variability from the perspective of predicting future ice sheet mass loss. To examine this, we compare the overall retreat of each glacier (defined as the difference between the mean values from 1993-1995 and 2010-2012) against the equivalent change in the five forcings. Again M_1 and M_2 provide the strongest correlation, giving R^2 values of 0.54 and 0.57 ($p < 0.01$) respectively, compared to 0.41 ($p < 0.01$) for T_O (Figure 5e-h; Table S3). There is no significant correlation between the magnitude of the overall change in P and T_A and Q at $p < 0.05$, with the northern glaciers again showing a much smaller retreat for a given increase in the atmospheric forcing.

Discussion

Our findings demonstrate that the timing and magnitude of tidewater glacier retreat along Greenland's east coast can be effectively explained as a combined linear response to atmospheric and oceanic conditions. Whilst variation in runoff alone can explain a large proportion of glacier retreat at individual glaciers (Figure 4), the sensitivity of this relationship is much stronger in southeast Greenland where ocean waters are warmer (and continued to warm more rapidly over the study period) compared to northeast Greenland (Figure 5a-b,f-g). It may thus be that contact with warm ocean waters preconditions the southern glaciers to greater sensitivity to changes in atmospheric temperature and hence runoff – if the ocean temperature is close to the *in situ* melting point, this will limit the potential for submarine melting, irrespective of the vigour of runoff-driven circulation. Whilst previous studies have hypothesised that regional differences in glacier stability in east Greenland may be linked to the strong latitudinal ocean temperature gradient (Seale et al., 2011, Walsh et al., 2012) and that a combined warming of ocean and atmosphere may provide the key trigger for rapid glacier retreat (Bevan et al., 2012, Christoffersen et al., 2012), we are able to demonstrate quantitatively that the combined influence of ocean and atmospheric temperature provides the strongest predictor of both spatial and temporal variation in glacier terminus position (Figure 5). In this way, our results agree with recent observations from the Antarctic Peninsula which show that, while there has been a strong atmospheric warming trend in this region, the magnitude of glacier retreat is much greater in areas where glaciers are in contact with warm Circumpolar Deep Water (Cook et al., 2016). While the existence of a correlation cannot alone provide conclusive evidence of a causal link, our results thus join a growing body of evidence indicating a role for both oceanic and atmospheric warming in driving the retreat of marine-terminating outlet glaciers.

Our results suggest that variability in terminus position across the 10 study glaciers can be parameterised as

$$\frac{dP}{dt} = a\,\frac{dM_1}{dt}, \qquad (1)$$

where t is time and a = -0.014±0.002 or -0.018±0.006 km / (m^3 s^{-1} °C) depending on whether the parameterisation is fitted to maximise agreement with the year-to-year variability (Figure 5d) or overall retreat (Figure 5i) respectively (Figure S3). This simple formulation effectively captures both the temporal variability in the rate of change of glacier front position and the widely differing magnitude of response at the different outlet glaciers (Figure 6). Across 10 glaciers, equation (1) can explain 54 % of year-to-year variability in terminus position (Figure 5d) and 54 % of variation in the overall retreat rate (Figure 5i). As such, while the prediction of individual tidewater glacier behaviour on timescales of a few years or less may require detailed glacier-specific knowledge of bedrock topography (e.g. Howat et al., 2008, Carr et al., 2013) and high-resolution modelling of ice dynamics (e.g. Todd et al., 2018), our results show that on longer timescales variation in the glaciers' terminus positions can be captured with much simpler parameterisations. These parameterisations translate the complex interaction of ice sheets with the atmosphere and ocean into simple yet statistically strong relationships that provide a new pathway for the inclusion of tidewater glacier retreat in the large-scale ice sheet models needed to predict global sea level rise (e.g. Fürst et al., 2015, Aschwanden et al., 2016).

This quasi-linear behaviour likely reflects the complex topography and thus relatively frequent occurrence of pinning points (such as lateral constrictions and submarine sills) within Greenlandic glacier-fjord systems. This means that, unlike regions of West Antarctica where bed topography may precondition the ice sheet to centennial scale unstable retreat (e.g. Joughin et al., 2014), change at many of Greenland's tidewater glaciers may occur as series of rapid short-lived retreats which collectively do not deviate far from the linear response to climate warming. Capturing the exact timing and magnitude of these steps is difficult and may not be necessary if the aim is to predict ice sheet mass loss on timescales of decades or longer. A good example of this can be seen when comparing KG and Helheim Glacier (HG): as the forcings increased between 2000 and 2005, HG retreated steadily whilst KG remained comparatively stable before undergoing a rapid ~ 5 km retreat between topographic pinning points in 2004-5 (Figures 3d-e and S1). If viewed over the period 2000 to 2005, the retreat of KG appears sudden while the retreat of HG appears prolonged; however, when considered over the full 20-year time series, both glaciers exhibited a broadly similar retreat between 2000-2005 with periods of comparative stability before and after.

This topographic influence accounts for some of the largest outliers in the relationship between P and M_1 (Figure 5d), with a ~3-4 km discrepancy between the observed and parameterised modelled terminus position briefly existing at KG due to the delayed response of this glacier to ocean/atmosphere warming during 2000-2005 (Figures 3e and 6a). At KG, this discrepancy is short-lived, but this observation illustrates how equation (1) is likely to be least effective at glaciers at which current behaviour is particularly strongly influenced by topography: for example, looking to west Greenland, Jakobshavn Isbræ may have been undergoing an unstable retreat into deeper water since the loss of its floating tongue in the late 1990s (Joughin et al., 2008), whilst the stability of Store Glacier to the north is attributed to the presence of an exceptionally prominent topographic pinning point (Todd et al., 2018). While such glaciers will ultimately adjust to a new climatically stable position, their terminus position may differ more strongly from the linear trend in the short term. Nevertheless, our findings suggest that simple formulations such as equation (1) can play an important role in parameterising the response to climate warming of many tidewater glaciers, including major outlets such as KG, HG and DJ.

The efficacy of this approach is likely to be dependent on the timeframe in question. The influence of topographic pinning points will be magnified on short timescales (~5 years or less), with this effect reduced when retreat rates are averaged over longer timescales. Furthermore, the slow response time of glaciers will modulate climatic signals by filtering out higher frequency variation – for example, this may explain the muted response of the southern glaciers to the short-lived cooling/warming over 2009-10 (Figure 2-3). At much longer timescales, glaciers will become less sensitive to the ocean as they retreat into shallower water and onto dry land, while evolving ice sheet mass balance and geometry will also likely impact upon the relationship between forcings and terminus position. We therefore suggest that the relationship described in equation (1) is most appropriate when considering processes on timescales of ~5-100 years, with uncertainty increasing either side of this window.

The dependency of retreat rate on both runoff and ocean temperature points to a key role for calving front processes in driving the retreat of Greenland's tidewater glaciers. The obvious link lies in submarine melting: theory and modelling suggest that submarine melt rate is dependent on both ocean temperature and runoff, with the latter driving buoyant plumes that increase the turbulent transfer of oceanic heat to glacier calving fronts (e.g. Jenkins, 2011, Xu et al., 2013). The role of submarine melting as a control on terminus position appears straightforward where glaciers are relatively slow flowing and warm ocean waters are capable of inducing submarine melt rates on par with ice velocity; in such circumstances undercutting by submarine melting may be the primary source of frontal ablation (Bartholomaus et al., 2013, Luckman et al., 2015), such that changes in terminus position are determined by the difference between ice velocity and submarine melt rate (Slater et al., 2017). The applicability of this mechanism at faster flowing glaciers is less clear however, as predictions of ice front-averaged submarine melt rates fall far below terminus velocities (Todd and Christoffersen, 2014, Rignot et al., 2016). Indeed, observations indicate a mechanistic difference between the small scale calving in submarine melt dominated systems (Luckman et al., 2015) and the massive buoyant calving of icebergs from Greenland's largest and fastest flowing glaciers (James et al., 2014). Nevertheless, our findings indicate that terminus position at these large and fast flowing glaciers also responds rapidly and predictably to variability in ocean/atmosphere forcing.

We also note that the lack of improvement in the correlation between P and M_2 (= $Q^{1/3}(T_O-T_f)$) compared to M_1 (= $Q(T_O-T_f)$) is at odds with the dependency expected if retreat rate was a direct function of submarine melt rate (Jenkins, 2011). It may be that this theoretical relationship (which is yet to be validated by field data) does not reflect the reality of the relationship between T_O, Q and submarine melting - for example, Slater *et al* (2016) report that the correct value for the exponent may be as high as ¾ under certain circumstances. Alternatively, the apparently simple relationship between *P* and M_1 may be the integrated result of not only submarine melting but also additional factors including ice mélange / sea ice coverage (e.g. Christoffersen et al., 2012, Moon et al., 2015) and hydrologically forced acceleration of ice motion (e.g. Sugiyama et al., 2011). The stronger correlations between *P* and *Q* rather than T_A (Figures 4 and 5) indicate that catchment-wide melt, and hence runoff, is of greater importance than local air temperatures at the terminus as a control on retreat rate. While this suggests that processes driven by local surface melting (e.g. through hydrofracture-driven calving) are of secondary importance, we cannot discount the possibility that our results reflect a more complex mix of processes related to basal hydrology, glacier dynamics, submarine melting and calving. Thus whilst our findings indicate that a combined ocean/atmosphere forcing is a key control on the stability of even large, fast flowing tidewater glaciers, further research is needed to identify and constrain the processes that link this forcing with frontal ablation and glacier retreat.

Over a 20-year period, we have observed a significant correlation between variability in glacier terminus position and a simple parameterisation that combines oceanic and atmospheric forcings at 10 tidewater glaciers along Greenland's east coast. Our results demonstrate that while increased melting and runoff in response to atmospheric warming can explain much of the temporal variability in glacier terminus position, the temperature of the adjacent ocean waters is also a strong determinant of the absolute magnitude of retreat. We find that even at very large and fast flowing glaciers like Kangerdlugssuaq Glacier and Helheim Glacier, where the nonlinear response to climate forcing has previously been emphasised, over timescales of a few years or longer, this forcing dominates over site-specific effects relating to the complexities of local topography. While topography remains an important factor in modulating the response of tidewater glaciers to climate, our findings nevertheless suggest that simple parameterisations linking terminus retreat to runoff and ocean temperature, suitable for inclusion in large-scale ice sheet models, have an important role to play in modelling the response of the Greenland ice sheet to atmospheric and oceanic warming.

Methods

Study glaciers

Details of the 10 study glaciers are given in Table S1. These glaciers represent a subset of the 32 glaciers documented by Seale *et al* (2011), chosen to span a range of conditions along the east coast of Greenland. Within each region, the largest outlet glaciers (with respect to ice velocity and terminus width; Table S1) were selected. In the far northeast of Greenland, the major outlet glaciers drain into substantial floating ice tongues (e.g. Wilson et al., 2017). Charting the retreat of these glaciers (where changes in grounding line position rather than calving front position are likely of primary importance) is not possible with the methods employed here, and so no glaciers were selected in this region.

Air temperature

Mean summer air temperature (Figure 2a-b), T_A, is based on the May-September mean of monthly temperatures from ERA-Interim global atmospheric reanalysis (Dee et al., 2011). For each glacier, temperatures are extracted from the reanalysis cell in which the terminus lies. To account for differing mean topography between cells, these values are adjusted to give sea level temperature assuming an atmospheric lapse rate of 0.0065 °C / m.

Runoff

Annual mean catchment runoff, *Q,* for each of the 10 glaciers (Figures 1 and 2c-d) is obtained from a 1 km surface melting, retention and runoff model forced with ERA-Interim and 20CR reanalyses (Wilton et al., 2017). Runoff due to basal melting is expected to be limited and is therefore not considered. Meltwater is routed through glacial catchments using the hydraulic potential gradient (Shreve, 1972) based on the ice surface and bed topography (Bamber et al., 2013). *Q* is predicted to be greatest at KG due to its large catchment area and more melt-favourable hypsometry relative to HG and DJ, which have comparable catchment areas (Figures 1 and 2c-d).

Ocean temperature

We seek to compare changes in glacier terminus position to a measure of ocean water temperature, T_O, in the fjords adjacent to the glaciers. Because there are few *in situ* hydrographic measurements from fjords, and the fjords are not well resolved in ocean circulation models, we define $T_O = T_R + c$, where T_R is ocean temperature based on reanalysis values for the continental shelf and *c* is a correction to account for temperature differences between the shelf and fjords.

T_R is obtained from the GLORYS2V3 1/4° ocean reanalysis product (Ferry et al., 2012). A decision must be made as to where to sample these data for each glacier. Because cross-shelf troughs are poorly mapped and not well resolved in the reanalysis, cells close to fjord mouths tend to be unrealistically shallow (e.g. Fenty et al., 2016) and so the warmer, deeper waters (crucial to the fjord heat budget) are not captured. Conversely, if the nearest cell of depth equal to that of the grounding line is chosen, this can be hundreds of kilometres away from the fjord mouth on the shelf break, and it is not clear that a pathway of such depth will exist between that cell and the glacier. As a compromise, we opt for the nearest cell of depth > 400 m, which is deep enough to sample the warmer Atlantic waters (AW) existing at depths greater than ~ 200 m whilst in many cases being located on the shelf rather than beyond the shelf break (Figure 1). For simplicity and consistency between glaciers, we take T_R as the annual mean temperature between 200-400 m (Figure 2e-f). This falls within the likely depth range of up-fjord currents (e.g. Cowton et al., 2016), and allows key inter-annual trends in AW temperature to be captured whilst reducing noise due to large seasonal variations in shelf surface water temperatures which likely have limited influence on the glaciers (Straneo and Heimbach, 2013).

To obtain values for the correction term *c,* we test these time series of T_R against available *in situ* observations from moorings and CTD surveys in the vicinity of T1 (Holfort et al., 2008, Murray et al., 2010), HG (Straneo et al., 2016), KG (Azetsu-Scott and Syvitski, 1999, Dowdeswell, 2004, Straneo et al., 2012, Inall et al., 2014) and, in the absence of data from the northern study glaciers, Nioghalvfjerdsbræ (NG) in the far north east of Greenland (Wilson and Straneo, 2015) (Figures 1 and S2). Fitting of T_R to the observations indicates that the reanalysis data overestimate *in situ* temperatures in these locations by approximately 1.5 °C (T1), 2.9 °C (HG), 3.1 °C (KG) and 0.3 °C (NG). While this may in part reflect errors in the reanalysis product (which is poorly constrained by observations on the shelf), significant cooling of AW is expected as it crosses the continental shelf from the core of the warm currents at the shelf break to the fjords (Straneo et al., 2012). To better represent the temperature of subsurface waters entering the fjords, we use these observations to adjust the values of T_R derived from the reanalysis data to give T_O. For the cluster of glaciers in southeast Greenland (M3, T1 and AB) we set c = 1.5 °C, while at HG and KG we set c = 2.9 °C and 3.1 °C respectively. For the glaciers in northeast Greenland (BG, VG, DJ, WG, HK), influenced by the same cooler recirculated AW as NG (Straneo et al., 2012), we set c = 0.3 °C. These offsets are then used to calculate the values of T_O used throughout the paper. While this adjustment is necessarily approximate given the scarcity of *in situ* observations, its application enables better representation of the temporal and spatial variability in the temperature of ocean water entering Greenland's fjords.

Terminus position

For the period 2000-2009, width-averaged changes in glacier terminus position *P* (expressed as distance from an arbitrary up-glacier location) are taken from Seale *et al* (2011) and based on the automated classification of all available MODIS imagery. We extend this time series by manual termini delineation (using the linear box method (Lea et al., 2014)) in Landsat scenes (e.g. Figure S1) at approximately monthly intervals over the period 2009-2015, and where available over the period

1990-1999. No Landsat scenes are available during the years 1991, 1993 and 1995. At KG, HG and DJ we supplement these data with terminus positions delimited using Envisat imagery by Bevan *et al* (2012).

Because the glaciers typically undergo an annual cycle of advance and retreat, error will be introduced into the mean annual position for glaciers and years where there are significant gaps in the available coverage. We therefore adjust glacier lengths according to

$$P = P_{mean} + \left(\frac{1}{2}\mu_a r\right), \tag{2}$$

where P is the adjusted mean annual terminus position, as based on P_{mean}, which is the mean of the available data for each year. r is the typical annual range in terminus positions for each glacier, based on the period 2010-2013 when continuous Landsat availability gives accurate near year-round coverage (Table S4). Each data point is given a weighting μ based on the month within which it falls, ranging linearly from 1 (October, when the termini are typically most retreated), to -1 (April, when the termini are typically most advanced). The mean weighting for each year, μ_a, thus provides an indication of the extent by which the available data points likely over or under estimate the true mean annual terminus position. For example, the only two data points for 1995 at DJ fall in August and September (when the glacier length will be close to its annual minimum). This gives μ_a = 0.5, and P is thus increased by 0.25 x r (= 0.3 km) with respect to P_{mean} to better approximate the true annual average terminus position. The difference between P_{mean} and P is shown in Figure 3 (being too small to plot in Figure 2g-h) and is in most cases negligible.

Statistics

Statistical comparison of T_A, Q, T_O, M_1 and M_2 with P is undertaken at the level of mean annual values. In Figure 5 (and Table S3) we consider data grouped from across the study glaciers, while in Figures 3 and 4 (and Table S2) we relate individual glacier-specific time series of anomalies in T_A, Q, T_O, M_1 and M_2 to those in P. Because these individual time series are in general non-stationary, classical linear regression may indicate a statistically significant correlation between variables in instances where in fact no relationship exists (Granger and Newbold, 1974). To reduce the risk of incorrectly interpreting such spurious relationships, we test for cointegration of the time series (Engle and Granger, 1987), a technique that has proven valuable in examining the relationships between non-stationary climate variables (e.g. Kaufmann and Stern, 2002, Mills, 2009, Beenstock et al., 2012). Cointegration occurs when a relationship between two or more non-stationary time series produces residuals that are themselves stationary, indicating a functional relationship that remains constant in time. A more thorough description of this approach, and its application in climate science, is provided by Kaufman and Stern (2002). We perform an Engle-Granger test for cointegration on each of the combinations of forcing and response time series using the *egcitest* function in Matlab R2016a (www.mathworks.com). Where linear regression indicates a significant correlation but cointegration is not established (at $p < 0.05$), we recognise the increased risk that this correlation may be spurious. All R^2 values given throughout the paper are significant at $p < 0.05$, with the specific p value given in each case, and all statistical values provided in Tables S2-3.

Acknowledgements

The authors would like to thank Adrian Luckman and Suzanne Bevan for providing glacier terminus position data, Edward Hanna, David Wilton and Philippe Huybrechts for providing surface melting and runoff data, Fiamma Straneo, Mark Inall and Stephen Dye for providing hydrographic data and the GLORYS project for providing ocean reanalysis data (GLORYS is jointly conducted by MERCATOR OCEAN, CORIOLIS and CNRS/INSU). This work was funded by NERC grants NE/K015249/1 and NE/K014609/1 to PN and AS respectively and a NERC studentship to DS.

Figures

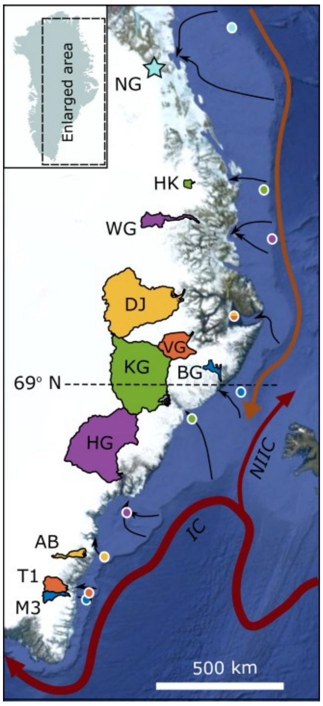

Figure 1. Map showing the location of the ten study glaciers (Table S1) in east Greenland: M3 = Mogens 3; T1 = Tingmjarmiut 1; AB = AP Bernstorffs Glacier; HG = Helheim Glacier; KG = Kangerdlugssuaq Glacier; BG = Borggraven; VG = Vestfjord Glacier; DJ = Daugaard-Jensen Glacier; WG = Waltershausen Glacier; HK = Heinkel Glacier. The location of Nioghalvfjerdsbræ (NG), which is referenced but does not constitute one of the study glaciers, is marked with a star. Hydrological catchments are shaded, and the divide between the northern and southern study glaciers at ~69° N is marked with the dashed line. The sample locations for ocean reanalysis temperature for the glaciers are shown as coloured circles. Also shown are the approximate locations of warm ocean currents (Straneo et al., 2012), with IC = Irminger Current and NIIC = North Iceland Irminger Current, and cross shelf troughs that may allow warm subsurface waters to access the study glaciers (black arrows; Jakobsson et al., 2012). The background image shows a satellite mosaic of Greenland with shaded sea floor bathymetry (Google Earth; Data: SIO, NOAA, U.S. Navy, NGA, GEBCO; Image: Landsat / Copernicus, IBCAO, U.S. Geological Survey).

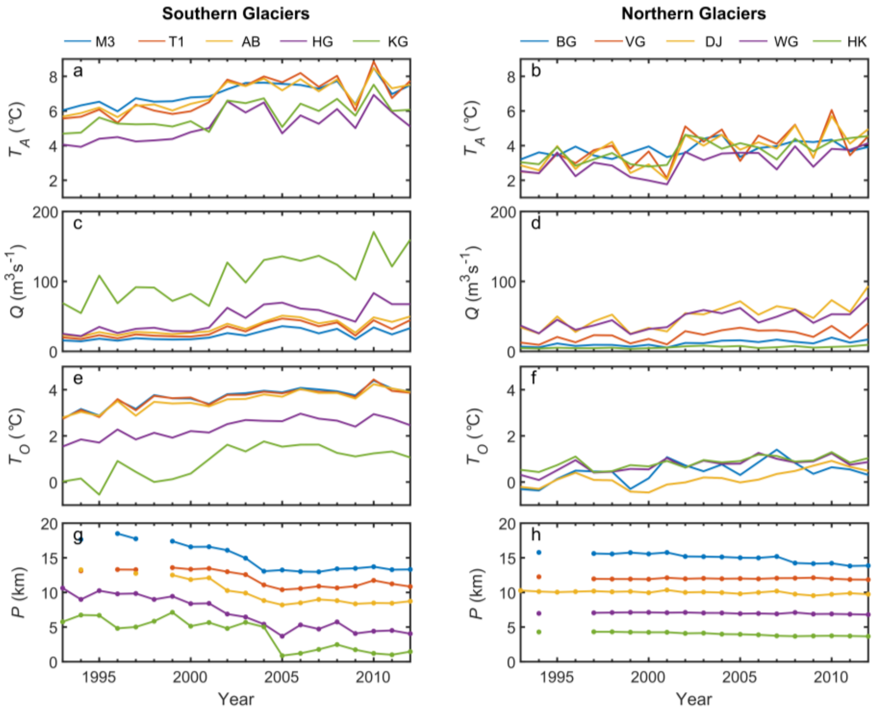

Figure 2. Annual average values of (a-b) air temperature (T_A), (c-d) runoff (Q), (e-f) depth-averaged subsurface ocean temperature (T_O) and (g-h) glacier terminus position (P), relative to an arbitrary up-glacier location, for the 10 study glaciers (Methods; Table S1). The left and right columns show glaciers south and north of ~69N respectively, and colours are as for Figure 1.

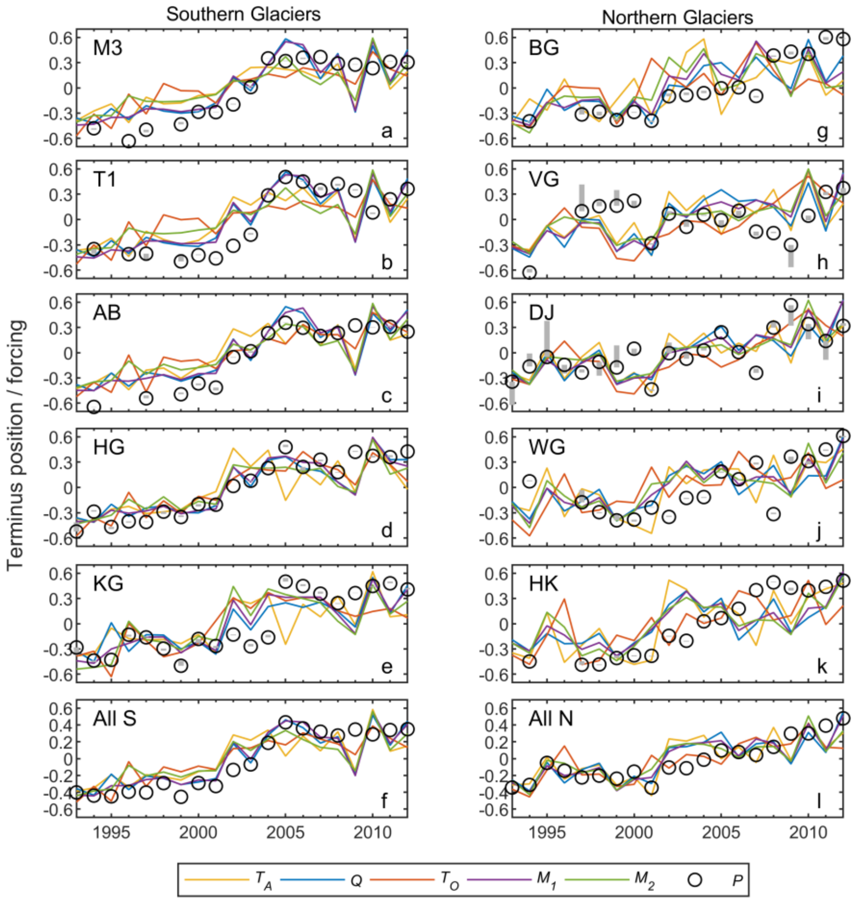

Figure 3. Time series of normalised anomalies in air temperature ($\tilde{T}_A$, orange) runoff ($\tilde{Q}$, blue), ocean temperature ($\tilde{T}_O$, red), $\tilde{M}_1$ (purple) and $\tilde{M}_2$ (green) and terminus position ($\tilde{P}$, black circles) for each glacier. Anomalies are expressed relative to the 20-year mean, and all values are normalised with respect to the observed range at that glacier. For ease of comparison, $\tilde{P}$ is shown inverted (i.e. positive change means retreat) and is in some cases discontinuous due to lack of observations. Vertical grey bars indicate the adjustment of P relative to P_{mean} (Methods).

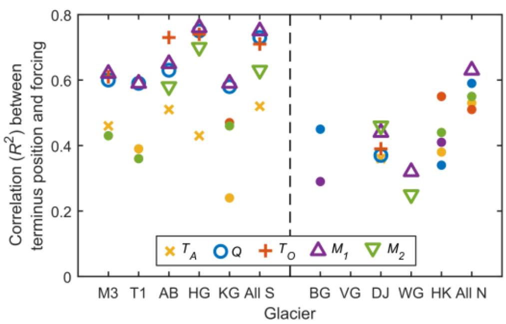

Figure 4. R^2 values for the relationship of terminus position (P) with air temperature (T_A) runoff (Q), ocean temperature (T_O) and M_1 *and* M_2 at each glacier and for the averaged regional southern ('All S') and northern ('All N') trends (Figure 3). Large markers show time series that are significantly

cointegrated at $p < 0.05$. Solid dots show instances which are correlated at $p < 0.05$, but are not cointegrated at this confidence level. No marker is shown where the time series are not significantly correlated or cointegrated. The dashed line separates the southern (left) and northern (right) glacier subsets. Statistical values are given in Table S2.

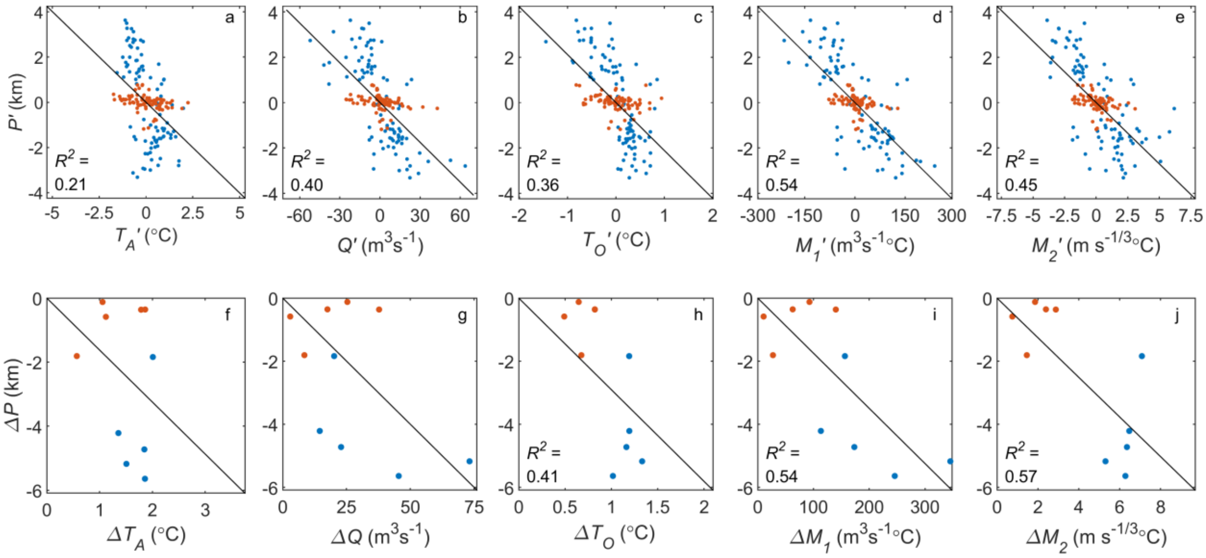

Figure 5. a-d. Relationship between anomalies in terminus position (P') and (a) air temperature (T_A') (b) runoff (Q'), (c) ocean temperature (T_O'), and ocean/atmosphere forcing (d) M_1' and (e) M_2'. Anomalies are shown relative to the 20-year mean at each glacier. f-j. Relationship between overall change in terminus position (ΔP) and (f) air temperature (ΔT_A), (g) runoff (ΔQ), (h) ocean temperature (ΔT), and ocean/atmosphere forcing (i) ΔM_1 and (j) ΔM_2. In each case, the overall change is calculated by subtracting the mean 1993-1995 value from the mean 2010-2012 value. On all plots, blue and red markers denote data from the southern and northern glaciers subsets respectively, and black lines show the best fit to all data. R^2 values (all significant at $p < 0.05$) are shown on all plots except (f) and (g), which are not significant at this level. Statistical values are given in Table S3.

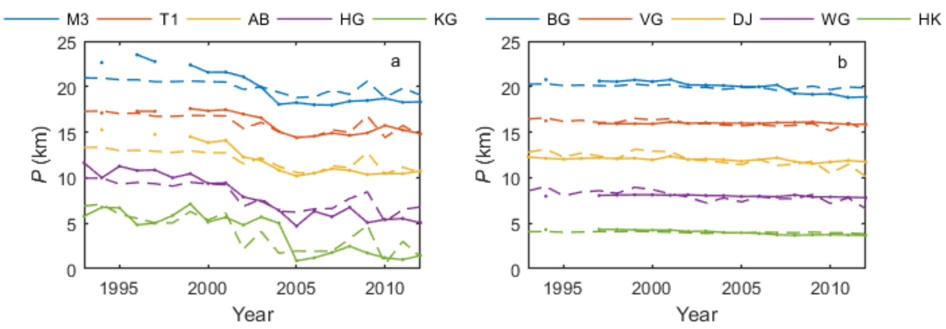

Figure 6. Change in terminus position P at the (a) southern glaciers and (b) northern glaciers, as observed (solid lines) and parameterised based on equation (1) (dashed lines). P is shown relative to an arbitrary up-glacier location, as in Figure 2e-f.

References

Aschwanden, A., Fahnestock, M. A. and Truffer, M. (2016) 'Complex Greenland outlet glacier flow captured', *Nature communications,* 7, pp. 10524.

Azetsu-Scott, K. and Syvitski, J. P. M. (1999) 'Influence of melting icebergs on distribution, characteristics and transport of marine particles in an East Greenland fjord', *Journal of Geophysical Research-Oceans,* 104(C3), pp. 5321-5328.

Bamber, J. L., Griggs, J. A., Hurkmans, R. T. W. L., Dowdeswell, J. A., Gogineni, S. P., Howat, I., Mouginot, J., Paden, J., Palmer, S., Rignot, E. and Steinhage, D. (2013) 'A new bed elevation dataset for Greenland', *Cryosphere,* 7(2), pp. 499-510.

Bartholomaus, T. C., Larsen, C. F. and O'Neel, S. (2013) 'Does calving matter? Evidence for significant submarine melt', *Earth and Planetary Science Letters,* 380, pp. 21-30.

Beenstock, M., Reingewertz, Y. and Paldor, N. (2012) 'Polynomial cointegration tests of anthropogenic impact on global warming', *Earth System Dynamics,* 3(2), pp. 173-188.

Benn, D. I., Cowton, T., Todd, J. and Luckman, A. (2017) 'Glacier calving in Greenland', *Current Climate Change Reports*, pp. 1-9.

Bevan, S. L., Luckman, A. J. and Murray, T. (2012) 'Glacier dynamics over the last quarter of a century at Helheim, Kangerdlugssuaq and 14 other major Greenland outlet glaciers', *Cryosphere,* 6(5), pp. 923-937.

Carr, J. R., Vieli, A. and Stokes, C. (2013) 'Influence of sea ice decline, atmospheric warming, and glacier width on marine-terminating outlet glacier behavior in northwest Greenland at seasonal to interannual timescales', *Journal of Geophysical Research-Earth Surface,* 118(3), pp. 1210-1226.

Carroll, D., Sutherland, D. A., Shroyer, E. L., Nash, J. D., Catania, G. A. and Stearns, L. A. (2017) 'Subglacial discharge-driven renewal of tidewater glacier fjords', *Journal of Geophysical Research: Oceans*.

Chauché, N., Hubbard, A., Gascard, J. C., Box, J. E., Bates, R., Koppes, M., Sole, A., Christoffersen, P. and Patton, H. (2014) 'Ice-ocean interaction and calving front morphology at two west Greenland tidewater outlet glaciers', *Cryosphere,* 8(4), pp. 1457-1468.

Christoffersen, P., O'Leary, M., Van Angelen, J. H. and van den Broeke, M. (2012) 'Partitioning effects from ocean and atmosphere on the calving stability of Kangerdlugssuaq Glacier, East Greenland', *Annals of Glaciology,* 53(60), pp. 249-256.

Cook, A., Holland, P., Meredith, M., Murray, T., Luckman, A. and Vaughan, D. (2016) 'Ocean forcing of glacier retreat in the western Antarctic Peninsula', *Science,* 353(6296), pp. 283-286.

Cowton, T., Sole, A., Nienow, P., Slater, D., Wilton, D. and Hanna, E. (2016) 'Controls on the transport of oceanic heat to Kangerdlugssuaq Glacier, east Greenland', *Journal of Glaciology*.

Dee, D. P., Uppala, S., Simmons, A., Berrisford, P., Poli, P., Kobayashi, S., Andrae, U., Balmaseda, M., Balsamo, G. and Bauer, d. P. (2011) 'The ERA-Interim reanalysis: Configuration and performance of the data assimilation system', *Quarterly Journal of the royal meteorological society,* 137(656), pp. 553-597.

Dowdeswell, J. (2004) *Cruise report - JR106b. RSS James Clark Ross. NERC Autosub Under Ice thematic programme. Kangerdlugssuaq Fjord and shelf, east Greenland*.

Engle, R. F. and Granger, C. W. J. (1987) 'Cointegration and error correction - representation, estimation and testing', *Econometrica,* 55(2), pp. 251-276.

Fenty, I., Willis, J. K., Khazendar, A., Dinardo, S., Forsberg, R., Fukumori, I., Holland, D., Jakobsson, M., Moller, D. and Morison, J. (2016) 'Oceans Melting Greenland: Early Results from NASA's Ocean-Ice Mission in Greenland', *Oceanography*.

Ferry, N., Parent, L., Garric, G., Drevillon, M., Desportes, C., Bricaud, C. and Hernandez, F. (2012) *Scientific Validation Report (ScVR) for Reprocessed Analysis and Reanalysis. MyOcean project report, MYO-WP04-ScCV-rea-MERCATOR-V1.0*.

Fried, M. J., Catania, G. A., Bartholomaus, T. C., Duncan, D., Davis, M., Stearns, L. A., Nash, J., Shroyer, E. and Sutherland, D. (2015) 'Distributed subglacial discharge drives significant submarine melt at a Greenland tidewater glacier', *Geophysical Research Letters,* 42(21), pp. 1944-8007.

Fürst, J., Goelzer, H. and Huybrechts, P. (2015) 'Ice-dynamic projections of the Greenland ice sheet in response to atmospheric and oceanic warming', *The Cryosphere,* 9(3), pp. 1039-1062.

Goelzer, H., Huybrechts, P., Fürst, J. J., Nick, F., Andersen, M. L., Edwards, T. L., Fettweis, X., Payne, A. J. and Shannon, S. (2013) 'Sensitivity of Greenland ice sheet projections to model formulations', *Journal of Glaciology,* 59(216), pp. 733-749.

Granger, C. W. and Newbold, P. (1974) 'Spurious regressions in econometrics', *Journal of econometrics,* 2(2), pp. 111-120.

Holfort, J., Hansen, E., Østerhus, S., Dye, S., Jonsson, S., Meincke, J., Mortensen, J. and Meredith, M. (2008) 'Freshwater fluxes east of Greenland', *Arctic-Subarctic Ocean Fluxes Defining the Role of the Northern Seas in Climate.,* 304.

Howat, I. M., Joughin, I., Fahnestock, M., Smith, B. E. and Scambos, T. A. (2008) 'Synchronous retreat and acceleration of southeast Greenland outlet glaciers 2000-06: ice dynamics and coupling to climate', *Journal of Glaciology,* 54(187), pp. 646-660.

Inall, M. E., Murray, T., Cottier, F. R., Scharrer, K., Boyd, T. J., Heywood, K. J. and Bevan, S. L. (2014) 'Oceanic heat delivery via Kangerdlugssuaq Fjord to the south-east Greenland ice sheet', *Journal of Geophysical Research: Oceans*, 119(2), pp. 631-645. Available at: http://onlinelibrary.wiley.com/doi/10.1002/2013JC009295/abstract (Accessed 01).

Jakobsson, M., Mayer, L., Coakley, B., Dowdeswell, J. A., Forbes, S., Fridman, B., Hodnesdal, H., Noormets, R., Pedersen, R. and Rebesco, M. (2012) 'The international bathymetric chart of the Arctic Ocean (IBCAO) version 3.0', *Geophysical Research Letters,* 39(12).

James, T. D., Murray, T., Selmes, N., Scharrer, K. and O'Leary, M. (2014) 'Buoyant flexure and basal crevassing in dynamic mass loss at Helheim Glacier', *Nature Geoscience,* 7(8), pp. 594-597.

Jenkins, A. (2011) 'Convection-Driven Melting near the Grounding Lines of Ice Shelves and Tidewater Glaciers', *Journal of Physical Oceanography,* 41(12), pp. 2279-2294.

Joughin, I., Howat, I. M., Fahnestock, M., Smith, B., Krabill, W., Alley, R. B., Stern, H. and Truffer, M. (2008) 'Continued evolution of Jakobshavn Isbrae following its rapid speedup', *Journal of Geophysical Research: Earth Surface,* 113(F4).

Joughin, I., Smith, B. E. and Medley, B. (2014) 'Marine Ice Sheet Collapse Potentially Under Way for the Thwaites Glacier Basin, West Antarctica', *Science,* 344(6185), pp. 735-738.

Kaufmann, R. K. and Stern, D. I. (2002) 'Cointegration analysis of hemispheric temperature relations', *Journal of Geophysical Research-Atmospheres,* 107(D1-D2).

Lea, J. M., Mair, D. W. F. and Rea, B. R. (2014) 'Instruments and Methods Evaluation of existing and new methods of tracking glacier terminus change', *Journal of Glaciology,* 60(220), pp. 323-332.

Luckman, A., Benn, D. I., Cottier, F., Bevan, S., Nilsen, F. and Inall, M. (2015) 'Calving rates at tidewater glaciers vary strongly with ocean temperature', *Nature Communications,* 6.

McFadden, E. M., Howat, I. M., Joughin, I., Smith, B. and Ahn, Y. (2011) 'Changes in the dynamics of marine terminating outlet glaciers in west Greenland (2000-2009)', *Journal of Geophysical Research-Earth Surface,* 116.

Mills, T. C. (2009) 'How robust is the long-run relationship between temperature and radiative forcing?', *Climatic change,* 94(3-4), pp. 351.

Moon, T., Joughin, I. and Smith, B. (2015) 'Seasonal to multiyear variability of glacier surface velocity, terminus position, and sea ice/ice mélange in northwest Greenland', *Journal of Geophysical Research: Earth Surface,* 120(5), pp. 818-833.

Murray, T., Scharrer, K., James, T. D., Dye, S. R., Hanna, E., Booth, A. D., Selmes, N., Luckman, A., Hughes, A. L. C., Cook, S. and Huybrechts, P. (2010) 'Ocean regulation hypothesis for glacier dynamics in southeast Greenland and implications for ice sheet mass changes', *Journal of Geophysical Research-Earth Surface,* 115.

Murray, T., Scharrer, K., Selmes, N., Booth, A. D., James, T. D., Bevan, S. L., Bradley, J., Cook, S., Llana, L. C., Drocourt, Y., Dyke, L., Goldsack, A., Hughes, A. L., Luckman, A. J. and McGovern, J. (2015) 'Extensive retreat of Greenland tidewater glaciers, 2000-2010', *Arctic Antarctic and Alpine Research,* 47(3), pp. 427-447.

Nick, F. M., Vieli, A., Andersen, M. L., Joughin, I., Payne, A., Edwards, T. L., Pattyn, F. and van de Wal, R. S. W. (2013) 'Future sea-level rise from Greenland's main outlet glaciers in a warming climate', *Nature,* 497(7448), pp. 235-238.

Rignot, E. and Kanagaratnam, P. (2006) 'Changes in the velocity structure of the Greenland ice sheet', *Science,* 311(5763), pp. 986-990.

Rignot, E., Xu, Y., Menemenlis, D., Mouginot, J., Scheuchl, B., Li, X., Morlighem, M., Seroussi, H., van den Broeke, M., Fenty, I., Cai, C., An, L. and de Fleurian, B. (2016) 'Modeling of ocean-induced ice melt rates of five west Greenland glaciers over the past two decades', *Geophysical Research Letters,* 43(12), pp. 6374-6382.

Seale, A., Christoffersen, P., Mugford, R. I. and O'Leary, M. (2011) 'Ocean forcing of the Greenland Ice Sheet: Calving fronts and patterns of retreat identified by automatic satellite monitoring of eastern outlet glaciers', *Journal of Geophysical Research-Earth Surface,* 116.

Shreve, R. L. (1972) 'Movement of water in glaciers', *Journal of Glaciology,* 11, pp. 205-214.

Slater, D., Goldberg, D., Nienow, P. and Cowton, T. (2016) 'Scalings for submarine melting at tidewater glaciers from buoyant plume theory', *Journal of Physical Oceanography,* in press.

Slater, D. A., Nienow, P. W., Goldberg, D. N., Cowton, T. R. and Sole, A. J. (2017) 'A model for tidewater glacier undercutting by submarine melting', *Geophysical Research Letters,* 44(5), pp. 2360-2368.

Straneo, F., Hamilton, G. S., Stearns, L. A. and Sutherland, D. A. (2016) 'Connecting the Greenland Ice Sheet and the Ocean: A case study of Helheim Glacier and Sermilik Fjord', *Oceanography,* 29(4), pp. 34-45.

Straneo, F. and Heimbach, P. (2013) 'North Atlantic warming and the retreat of Greenland's outlet glaciers', *Nature,* 504(7478), pp. 36-43.

Straneo, F., Heimbach, P., Sergienko, O., Hamilton, G., Catania, G., Griffies, S., Hallberg, R., Jenkins, A., Joughin, I., Motyka, R., Pfeffer, W. T., Price, S. F., Rignot, E., Scambos, T., Truffer, M. and Vieli, A. (2013) 'Challenges to Understanding the Dynamic Response of Greenland's Marine Terminating Glaciers to Oceanic and Atmospheric Forcing', *Bulletin of the American Meteorological Society,* 94(8), pp. 1131-1144.

Straneo, F., Sutherland, D. A., Holland, D., Gladish, C., Hamilton, G. S., Johnson, H. L., Rignot, E., Xu, Y. and Koppes, M. (2012) 'Characteristics of ocean waters reaching Greenland's glaciers', *Annals of Glaciology,* 53(60), pp. 202-210.

Sugiyama, S., Skvarca, P., Naito, N., Enomoto, H., Tsutaki, S., Tone, K., Marinsek, S. and Aniya, M. (2011) 'Ice speed of a calving glacier modulated by small fluctuations in basal water pressure', *Nature Geoscience,* 4(9), pp. 597-600.

Todd, J. and Christoffersen, P. (2014) 'Are seasonal calving dynamics forced by buttressing from ice melange or undercutting by melting? Outcomes from full-Stokes simulations of Store Glacier, West Greenland', *Cryosphere,* 8(6), pp. 2353-2365.

Todd, J., Christoffersen, P., Zwinger, T., Råback, P., Chauché, N., Benn, D., Luckman, A., Ryan, J., Toberg, N. and Slater, D. (2018) 'A Full-Stokes 3-D Calving Model Applied to a Large Greenlandic Glacier', *Journal of Geophysical Research: Earth Surface*.

Todd, J., Christoffersen, P., Zwinger, T., Råback, P., Chauché, N., Benn, D. I., Luckman, A., Ryan, J., Toberg, N., Slater, D. and Hubbard, A. (in press) 'A Full-Stokes 3D Calving Model applied to a large Greenlandic Glacier', *Journal of Geophysical Research: Earth Surface*.

van den Broeke, M., Box, J., Fettweis, X., Hanna, E., Noël, B., Tedesco, M., van As, D., van de Berg, W. J. and van Kampenhout, L. (2017) 'Greenland Ice Sheet Surface Mass Loss: Recent Developments in Observation and Modeling', *Current Climate Change Reports*, pp. 1-12.

Vieli, A., Jania, J. and Kolondra, L. (2002) 'The retreat of a tidewater glacier: observations and model calculations on Hansbreen, Spitsbergen', *Journal of Glaciology,* 48(163), pp. 592-600.

Walsh, K., Howat, I., Ahn, Y. and Enderlin, E. (2012) 'Changes in the marine-terminating glaciers of central east Greenland, 2000–2010', *The Cryosphere,* 6(1), pp. 211-220.

Wilson, N., Straneo, F. and Heimbach, P. (2017) 'Satellite-derived submarine melt rates and mass balance (2011–2015) for Greenland's largest remaining ice tongues', *The Cryosphere,* 11(6), pp. 2773-2782.

Wilson, N. J. and Straneo, F. (2015) 'Water exchange between the continental shelf and the cavity beneath Nioghalvfjerdsbrae (79 North Glacier)', *Geophysical Research Letters,* 42(18), pp. 7648-7654.

Wilton, D. J., Jowett, A. M. Y., Hanna, E., Bigg, G. R., Van Den Broeke, M. R., Fettweis, X. and Huybrechts, P. (2017) 'High resolution (1 km) positive degree-day modelling of Greenland ice sheet surface mass balance, 1870–2012 using reanalysis data', *Journal of Glaciology,* 63(237), pp. 176-193.

Xu, Y., Rignot, E., Fenty, I., Menemenlis, D. and Flexas, M. M. (2013) 'Subaqueous melting of Store Glacier, west Greenland from three-dimensional, high-resolution numerical modeling and ocean observations', *Geophysical Research Letters,* 40(17), pp. 4648-4653.